Diffusion of Lithium in α-Sn and β-Sn as Anode Materials for Lithium Ion Batteries

Jianjian Shi[*], Wenwu Shi, Wei Jin, Guangqiang Yin

School of Physical Electronics, Joint Laboratory for Police Equipment Research, University of Electronic Science and Technology of China, Chengdu, 610054, P.R. China
[*]E-mail: jlper@uestc.edu.cn

The diffusion behavior of lithium in the α-Sn and β-Sn were investigated using density function theory (DFT). The diffusion barrier of single lithium atom in the α-Sn is 0.21 eV, which shows a little change as another lithium atom was next to it. However, the barrier is 0.39eV for lithium in the β-Sn and the lithium tend to bond together when more lithium atoms appear. The different behavior of diffusion barriers are attributed to a different binding energy of Li-Li atoms in Sn with the different crystal structures. The α-Sn used as an anode material for lithium ion batteries is preferable to β-Sn for the fast diffusion of lithium.

1. INTRODUCTION

Rechargeable ion batteries were widely used in the area of electrochemical energy storage due to their high energy density. They have successfully used in portable electronic devices, and also can be used in electric vehicles (EVs), plug-in hybrid vehicles (PHVs), power grids and implantable medical devices. So far, various rechargeable ion batteries have been developed as energy storage, such as magnesium ion batteries (MIBs) [1,2], sodium ion batteries (NIBs) [3,4], lithium ion batteries (LIBs) [5-7]. In comparison with MIBs, the advantages of the LIBs are facile delithiation/lithiation in cathode/anode electrode [8]. Although the NIBs represent one of the most promising candidates owe to its low cost, abundance, NIBs is confined by a poor electrochemical performance[9]. Therefore, LIBs are still the dominant rechargeable energy storage up to now.

Although the LIBs show the fascinating sides, yet the performance of LIBs still need to be improved. Their energy density, cycle life and rate capability still remain insufficient to satisfy

automobile energy usage and especially space requirements like these high power equipments. To satisfy the high power equipment, the search for better electrode materials with more excellent performances still remains to be a big challenge. Group-IVA elements from the periodic elements table (C, Si, Ge, Sn and Pb) are promising anode materials, Sn has attracted much attention for both high storage capacity and low voltage operation[10]. The main problem in commercialization of LIBs with Sn anodes is large volume changes between delithiated phase (pure Sn) and fully lithiated phase ($Li_{4.4}Sn$) [11]. Many efforts have been devoted to restricting the volume change by reducing Sn particle size to nanoscale-size [12-14], dispersing nano-Sn in a conductive matriax, such as graphene, graphite, and carbon nanotubes[15-19], or alloying with metals (e.g., Sn-M, M=inactive Ni, Cu, Co)[20,21]. The above mentioned techniques and methods are well-established and can be used to achieve good electrochemical behavior of Sn anode. Such as 5 nm-Sn/C showed an initial discharge capacity of 1014 $mAh \cdot g^{-1}$ and a capacity retention of 722 $mAh \cdot g^{-1}$ after 200 cycles at the current density of 0.2 $A \cdot g^{-1}$[19]. Sn nanoparticles uniformly dispersed in a spherical carbon matrix has been synthesized by a spray pyrolysis technique, showing a capacity of 710 $mAh \cdot g^{-1}$ after 130 cycles at 0.2 $A \cdot g^{-1}$[22].

Many electrode materials show phase transformation upon lithium extraction and insertion, which induces the fading of electrochemical performance. Although those researches have been successful by focusing on retarding the volume expansion to improve the capacity of the Sn anode, less effort has been expended on understanding the effect of phase transformation on the electrochemical behavior. Sn shows several different crystal structures depending on the pressure and temperature. At atmospheric pressure and temperature below 286 K, a diamond structure (α-Sn or grey Sn) is preferred[23]. α-Sn transforms to the β-Sn (or white Sn) upon increasing the temperature or pressure. α-Sn and β-Sn are zero band gap semiconductor and metallic materials, respectively. The α-Sn is fragile and is easily cracked to expose surfaces of high gloss and having the general appearance of broken germanium, which is in comparison to the dull appearance of surfaces exposed when transformed tin is broken. Researchers found that during delithiation, β-Sn as anode materials for the LIBs can be transform into α-Sn. Moreover, at ambient temperature the α-Sn is stable[24]. Knowing about the Li diffusion mechanism in the α-Sn and β-Sn would contribute to the development of the LIBs with a higher capacity density.

Since the first theoretical prediction on a phase transition from semiconducting face center cubic silicon to a metallic phase at high pressure and the later experimental confirmation in early 1980s, computational electronic theory has matured into a powerful complementary tool for research in materials science. Subsequently, the computer simulation method occurs so as to it is really facile for the anticipation of architectures as well as performances of new materials, in particular at the atomic scale. Numerical simulations have not only reproduced experimental observations, but also provided an atomistic description of the process to help in understanding the underlying phenomenon. Computer simulations have also been applied to lithium ion batteries research program, such as the first-principles calculations (ab initio) based on the density functional theory (DFT) have been successfully applied to predict all kinds of vital performances of the LIBs, such as operating voltage, capacity and so on. Moreover, there are few theoretical studies on the mechanism using first principles based on the DFT calculations such as the intrinsic diffusion mechanism of Li ion for the LIBs. In this

report, we calculated the total energy via calculating energy changes along a pathway to assess diffusion barriers. Our main purpose is to study on the diffusion mechanism of Li the α- and β-Sn, so that we can make contributions to manufacture the preferable the LIBs which satisfy recent demands on energy and environmental sustainability.

2. COMPUTATION DETAILS

All the simulations were performed using the first-principles calculations based on density functional theory (DFT) as implemented in VASP code. The Perdew-Burke-Ernzerhof (PBE) generalized gradient approximation and the projector augmented wave (PAW) method [26] were used to describe exchange-correlation energy and electron-ion interactions, respectively, and an energy cutoff of 450 eV was used. The 64-atoms supercell and $3\times3\times3$ k-point mesh in the scheme of Monkhorst-Pack for Brillouin zone sampling [27] were applied for the α-Sn. And 108-atom supercell and $3\times3\times5$ grid was applied for β-Sn. All atoms were fully relaxed using the conjugate gradient approximation (GGA) until the force on every atom is smaller than 0.02 eV/Å.

In our calculation, the diffusion path and the transition states were evaluated by the climbing-image nudged-elastic-band (CI-NEB) method [28]. Several intermediate states can generate by linear interpolation method only upon our given the initial and final states so as to find the saddle points

3. RESULTS AND DISCUSSION

The crystal structures of α-Sn and β-Sn are shown in Fig.1 (a) and (b), respectively. The calculated lattice constants of the two phases were calculated to be 6.654 Å and 5.935 Å (c/a=0.543) for α-Sn and β-Sn, respectively. We find that the lattice constants determined with PBE and GGA agree well with the experimental values 6.480Å[29]and 5.831Å (c/a=0.545)[30].The mass density of α-Sn is roughly 20 percent smaller than that of β-Sn. The Sn-Sn bond lengths are 3.075 and 2.881 Å for α-Sn and β-Sn respectively.

The stable positions of single-Li atoms in the α- and β-Sn were investigated. It was observed that the tetrahedral interstitial sites are the most stable sites of lithium interstitial in the α-Sn via a geometry optimization, as shown by the green balls in Fig. 1 (c). The bond length between four closest tin and the Li interstitial atom is 2.963 Å, and the six second closest tin and Li atoms is 3.384 Å, which is analogous to phenomena between lithium and sodium atoms in the silicon crystal structure[31]. The most stable site of single-Li interstitial in the β-Sn is presented with by the green ball in Fig. 1 (d), surrounded by seven tin atoms with bond distances of ~2.69-2.98 Å. The moving pathway of single-Li atom is by transferring from one stable site to the nearest stable one by passing a transition site. Because of structure difference between the α- and β-Sn, there are different diffusion pathways in them: Li interstitial pass through the hexagonal positions and the rhombus interstitial position in the α- and β-Sn, respectively, as represented in the insert of Fig.2 at relative diffusion coordinates of 0.5.
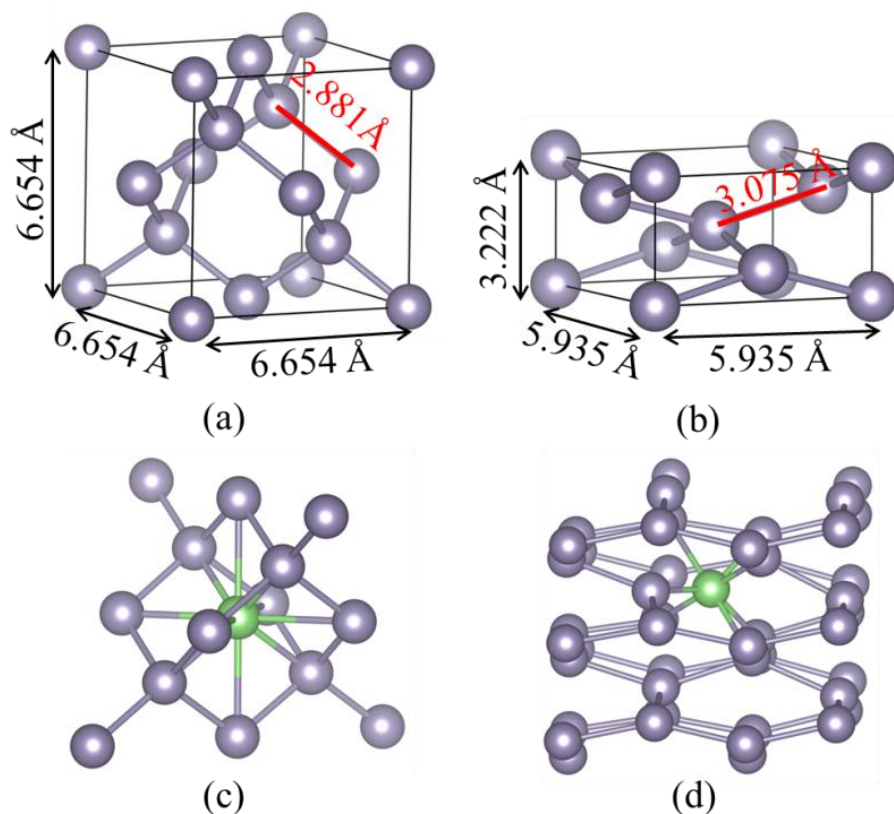
Figure 1. Crystalline structure of (a) α-Sn with a diamond structure and (b) β-Sn with a tetragonal structure. Transition positions of the Li in (c) α- and (d) β-Sn lattices are shown. The medium purple and green balls represent Sn and Li atoms, respectively.

In α-Sn, the diffusion path involves a hexagonal site as a transition site, at which Li is surrounded by six neighbor Sn atoms with Li-Sn bond length of 2.84 Å, and this structure corresponds to consisting of two parallel triangles being perpendicular to the diffusion pathway. In β-Sn, Li pass through a rhombus interstitial sites, at which Li has two nearest-neighbor Sn atoms and two second-nearest-neighbor Sn atoms, the Li-Sn bond lengths are 2.575 Å and 2.728 Å, respectively.

The diffusion energy curves of isolated Li atom from one stable position to a neighboring one in the α- and β-Sn are represented in Fig. 2 (a) and (b) (i.e., the red dotted line), respectively. The atomic configurations of stable and transition state are shown in Fig. 2. For the isolated Li diffusion, with represents the low Li concentration so that the Li atom circled by a black ring does not appears. The diffusion barrier is 0.21 eV of an isolated Li interstitial in the α-Sn and 0.389eV in β-Sn. The low barrier of Li atom in the α-Sn indicates that Li diffuses in the α-Sn at a Li. The Li-Sn bond lengths are 2.84 Å, and 2.575 Å, 2.728 Å in α- and β-Sn as Li locates at the transition states, respectively, according to the above results. The space for Li diffusion is larger in α-Sn than in β-Sn, so the diffusion barrier is smaller for Li diffusion in α-Sn.
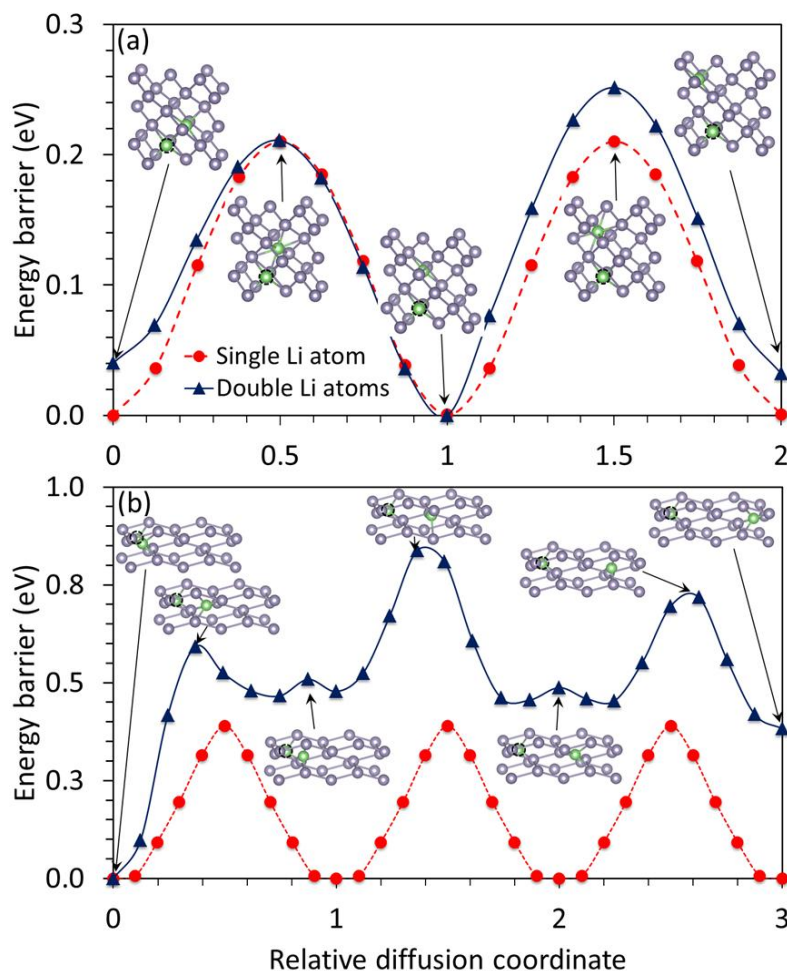
Figure 2. The diffusion energy curves of isolated Li atom from one stable position to a neighboring one in the (a) α- and (b) β-Sn. The dotted line is the energy curve for an isolated Li and the solid line is the energy curve for the diffusion of Li with the addition of a second Li atom. The atomic structure of transition states are shown as insets.

It is evident that the diffusion of an individual Li atom is easy in both of the α-Sn and β-Sn. However, much more Li atoms will emerge in the structure during charging. Meanwhile, the Li-Li interaction was considered that would influence the diffusion rate of the Li atoms. Hence, the diffusion barrier of Li atom was investigated with an additional Li atom (which was circled by a black dotted circle) was placed close the initial diffused Li atom. Fig. 2 (a) and (b) show the diffusion energy barrier curves of the Li in the α- and β-Sn. It shows different diffusion behavior of Li α- and β-Sn with another Li atom appears close the original diffused Li interstitial. The diffusion barrier decreases by 0.04 eV as moving from position 0 to position 1 for Li and from position 0 to position 2, the diffusion energy barrier increases by 0.04 eV in the α-Sn. This is a good example of a synergetic diffusion. When two Li atoms are placed next to each other, with the decrement of energy barrier, the diffusion phenomenon started to occur. The similar phenomena have been observed of magnesium and lithium diffusion process in silicon lattices [31,32]. The diffusion of the initial Li interstitial from position 1 to position 2 does not be affected by the second extra lithium atom placed owe to the Li insertion gives

rise to the localized lattice distortions, influence of Li-Li interaction will weaken fast with increasing the distance between the Li atoms. While it is noted that with another lithium atom was placed, the energy barrier increases from 0.389 to 0.838eV as the Li atoms move from position 0 to position 2 in the β-Sn (as represented in Fig. 2 (b), increased by 0.45 eV. It is demonstrated that more Li atoms are placed in the α-Sn which had almost no effects on the diffusion of Li atom; more Li atoms are placed in which severely hampered the diffusion of Li atoms.
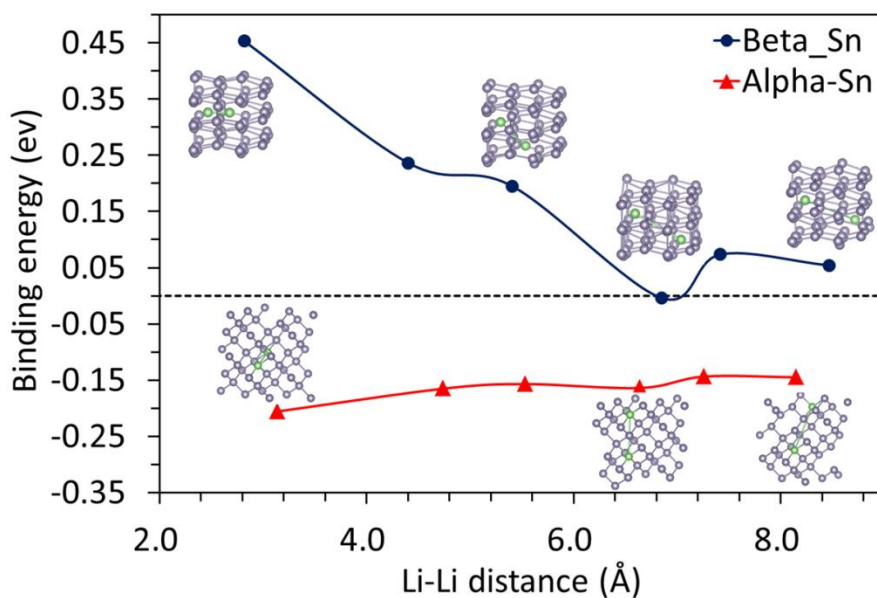

Figure 3. Change of binding energy curves of with Li-Li distances.

In order to research for the reason why the diffusion barrier increases in β-Sn with the addition of a second Li atom, we calculated the binding energy (E_b) by the following equation:

$$E_b = 2H_f(\text{Li}_I) - H_f(\text{Li} - \text{Li}) \qquad (1)$$

$H_f(\text{Li-Li})$ and $H_f(\text{Li}_I)$ represent the formation energy of the Li-Li complex and the isolated lithium atom formation energy in tin, respectively. A positive E_b indicates that it is easy to form Li-Li complex upon lithium atoms exits in the white tin. Fig. 3 shows the change of binding energy with Li-Li distances. All E_b is negative when two lithium atoms are at the stable sites in the α-Sn. While almost all E_b are larger than 0 eV, for examples the binding energy is 0.45 eV at the 2.82 Å. It is shown that the binding energy is larger than in the grey tin at the same Li-Li distances. From Figure 3, in the grey tin, we observed that the binding energies only have a little increase from 2.0 to 8.5 Å, which manifests that Li-Li interaction is very weak, so that we can draw a conclusion that lithium atoms are not easy to form clusters in the α-Sn. However, there is an opposite phenomenon in the β-Sn: lithium atoms are tends to form clusters. This result agrees the above dynamic simulation result.

The performance of the LIBs is significantly dependent on the properties of the constituent materials, in particular on the electrochemical properties of the cathode and anode materials [33]. The energy density is determined by the material's properties, such as reversible capacity and operating

voltage, which are generally determined by the material chemistry, i.e., effective redox couples and maximum lithium concentration in active materials [33]. The rate capability and cycling performances are determined by the electronic and ionic motilities in the electrode materials. From the above results we can see that the α-Sn is better to be used as high rate capability anode material for LIBs

4. CONCLUSION

In conclusion, the diffusion behavior of the Li atoms in the α-Sn and in the β-Sn was studied by using density functional theory. The diffusion barrier of single lithium atom in the α-Sn is 0.21 eV, which shows a little change as another lithium atom was next to it. However, the barrier is 0.39eV for lithium in the β-Sn and the lithium tend to bond together when more lithium atoms appear. So the diffusion barriers of Li atoms either increase or decrease in α- and β-Sn, respectively, when another Li atom occurs on next to the initial single-Li interstitial. The α-Sn can be a promising alternative candidate than the β-Sn to be served as anode electrode materials for the LIBs.

References

1. P. Novák, R. Imhof and O. Haas, *Electrochimica Acta* 45 (1999) 351.
2. Z. Wang, Q. Su and H. Deng, *Physical Chemistry Chemical Physics* 15 (2013) 8705.
3. N. Bucher, S. Hartung, A. Nagasubramanian, Y.L. Cheah, H.E. Hoster and S. Madhavi, *Acs Applied Materials & Interfaces* 6 (2014) 8059.
4. Y. Jiang, M. Hu, D. Zhang, T. Yuan, W. Sun, B. Xu and M. Yan, *Nano Energy* 5 (2014) 60.
5. K. Amine, R. Kanno and Y. Tzeng, *Mrs Bulletin* 39 (2014) 395.
6. S. Goriparti, E. Miele, F. De Angelis, E. Di Fabrizio, R.P. Zaccaria and C. Capiglia, *Journal Of Power Sources* 257 (2014) 421.
7. A.D. Roberts, X. Li and H. Zhang, *Chemical Society Reviews* 43 (2014) 4341.
8. E. Yoo, J. Kim, E. Hosono, H.-s. Zhou, T. Kudo and I. Honma, *Nano Letters* 8 (2008) 2277.
9. K.B. Hueso, M. Armand and T. Rojo, *Energy & Environmental Science* 6 (2013) 734.
10. V.L. Chevrier and G. Ceder, *Journal of the Electrochemical Society* 158 (2011) A1011.
11. L.Y. Beaulieu, K.W. Eberman, R.L. Turner, L.J. Krause and J.R. Dahn, *Electrochemical And Solid State Letters* 4 (2001) A137.
12. M. Wu, X. Li, Q. Zhou, H. Ming, J. Adkins and J. Zheng, *Electrochimica Acta* 123 (2014) 144.
13. L. Bazin, S. Mitra, P.L. Taberna, P. Poizot, M. Gressier, M.J. Menu, A. Barnabe, P. Simon and J.M. Tarascon, *Journal Of Power Sources* 188 (2009) 578.
14. G. Saito, C. Zhu and T. Akiyama, *Advanced Powder Technology* 25 (2014) 728.
15. F.R. Beck, R. Epur, D. Hong, A. Manivannan and P.N. Kumta, *Electrochimica Acta* 127 (2014) 299.
16. M. Wu, C. Wang, J. Chen, F. Wang and B. Yi, *Ionics* 19 (2013) 1341.
17. P. Lian, J. Wang, D. Cai, G. Liu, Y. Wang and H. Wang, *Journal Of Alloys And Compounds* 604 (2014) 188.
18. X. Zhou, J. Bao, Z. Dai and Y.-G. Guo, *Journal Of Physical Chemistry C* 117 (2013) 25367.

19. Z. Zhu, S. Wang, J. Du, Q. Jin, T. Zhang, F. Cheng and J. Chen, *Nano Letters* 14 (2014) 153.
20. S. Liu, Q. Li, Y. Chen and F. Zhang, *Journal Of Alloys And Compounds* 478 (2009) 694.
21. Y.-S. Lin, J.-G. Duh and H.-S. Sheu, *Journal Of Alloys And Compounds* 509 (2011) 123.
22. Y. Xu, Q. Liu, Y. Zhu, Y. Liu, A. Langrock, M.R. Zachariah and C. Wang, *Nano Letters* 13 (2013) 470.
23. G.A. Busch, R. Kern, Solid State Physics, Academic, New York, 1960.
24. L. Xu, C. Kim, A.K. Shukla, A. Dong, T.M. Mattox, D.J. Milliron and J. Cabana, *Nano Letters* 13 (2013) 1800.
25. G. Kresse and J. Furthmuller, *Computational Materials Science* 6 (1996) 15.
26. G. Kresse and D. Joubert, *Phys. Rev. B* 59 (1999) 1758.
27. J.D. Pack and H.J. Monkhorst, *Phys. Rev. B* 16 (1977) 1748.
28. G. Henkelman, B.P. Uberuaga and H. Jonsson, *J. Chem. Phys.* 113 (2000) 9901.
29. R.F.C. Farrow, D.S. Robertson, G.M. Williams, A.G. Cullis, G.R. Jones, I.M. Young and P.N.J. Dennis, *Journal of Crystal Growth* 54 (1981) 507.
30. E.R. Jette and F. Foote, *The Journal of Chemical Physics* 3 (1935) 605.
31. O.I. Malyi, T.L. Tan and S. Manzhos, *Applied Physics Express* 6 (2013).
32. O.I. Malyi, T.L. Tan and S. Manzhos, *Journal Of Power Sources* 233 (2013) 341.
33. Y.G. Guo, J.S. Hu and L.J. Wan, *Adv. Mater.* 20 (2008) 2878.